



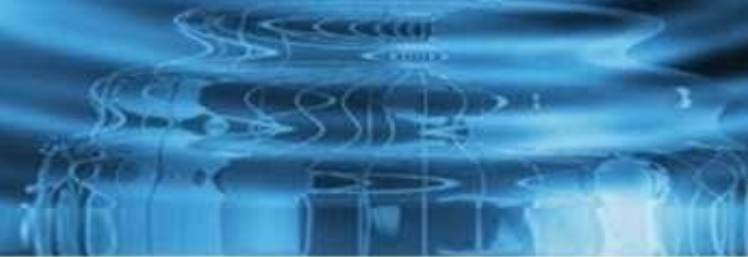
**IJITCE**

**ISSN 2347- 3657**

# **International Journal of**

## **Information Technology & Computer Engineering**

[www.ijitce.com](http://www.ijitce.com)



**Email : [ijitce.editor@gmail.com](mailto:ijitce.editor@gmail.com) or [editor@ijitce.com](mailto:editor@ijitce.com)**

## **ANALYZING THE IMPACT OF ADDITIVE MANUFACTURING ON THE MICROSTRUCTURE AND MECHANICAL PROPERTIES OF ALSi10MG**

<sup>1</sup>TALLOORI SAI KUMAR,<sup>2</sup>PERAM RAGHU,<sup>3</sup>YANAKAPATI KRISHNA,<sup>4</sup>T. VASANTHA DEVI

<sup>123</sup>Assistant Professor,<sup>4</sup>Student

*Department Of Mechanical Engineering*

*Abdul Kalam Institute of Technological Sciences, Kothagudem, Telangana*

### **ABSTRACT:**

When it comes to creating intricate and one-of-a-kind components using Additive Manufacturing (AM), Selective Laser Melting (SLM) is the better method than layer-by-layer melting. The goal of this effort is to generate highly dense AlSi10Mg alloy components by optimizing the SLM method. Scanning electron microscopy (SEM) and optical microscopy were used to analyze the specimens produced by AM for macro and micro structural issues, respectively. Additionally, an analysis was conducted to determine how layer thickness affected the mechanical properties of AlSi10Mg alloy components, including microhardness and ultimate tensile strength (UTS). A microstructure investigation revealed distinct microstructure shapes and behaviors at the boundary of the deposited layer's melt pool and further into the layer. As layer thickness reduced, tensile strength increased from 60 m to 30 m, most likely as a result of enhanced surface shape, ultra-fine cellular dendritic microstructure, and reduced porosity. In comparison to samples with a layer thickness of 60 m, samples with a layer thickness of 30 m showed a 24% increase in UTS when evaluated horizontally.

**Keywords:** density, layer thickness, UTS, microstructures, AlSi10Mg, SLM, and ultrathin films;

### **I. INTRODUCTION**

In recent years, SLM is considered to be one of the most promising technology in various sectors of aerospace and medical industries where the use of parts with complex geometries and light weight and strength of the material demand [1-3]. Unlike conventional manufacturing techniques, Additive manufacturing is a layer-by-layer manufacturing and joining technology to generate a 3D object. In this technique, a layer of metal powder first deposited and then the laser is irradiated on the metal powder causing melting and followed by rapid solidification. The exposure period of laser-material interaction will be in the range of few milliseconds. Thus, AM process is considered to be the high laser power-density with shorter interaction time [5-8]. AM of Al alloy powders have some challenges due to its superior thermal conductivity as well as high reflectivity. Therefore, resultant laser power required to melt Al alloy powder significantly enhanced. Moreover, porosity formation in the Al alloys is more common due to entrapment of oxide inclusions via oxidation resulting in weak spots in the AM built.

The SLM process is characterized by the extremely significant rapid melting and solidification. This influence the mechanical properties of the material and their study needs to be addressed.

Kempen k [4,8], reported that the extremely fine microstructure of AlSi10Mg parts can be produced by SLM technique with a controlled texture. In this study the AlSi10Mg alloy is additively manufactured to study and evaluate the microstructure, hardness, tensile strength and compare the results with the literature whether it can produce the similar properties obtained by heat treatments, coating of the surface, platform temperature, variation in process parameters, for two different layer thickness 60 $\mu$ m and 30 $\mu$ m, hence reducing cost and time of production.

## II. EXPERIMENTAL METHODS

The experiments were carried out using selective laser melting (Model: SLM 280HL) powder-bed AM machine using commercially available AlSi10Mg aluminium alloy powder. The chemical composition of AlSi10Mg alloy powder utilized in the current study is presented in Table 1. Particle size distribution was in the range of 20 - 70  $\mu$ m. The SLM 280HL system equipped with Ytterbium fiber laser (max. laser power - 400 W) with a spot size of 80  $\mu$ m (dia). Laser power used in the current study was 170 – 250 W and the process scanning speed was 500 – 700 mm/s. Two different layer thicknesses such as 30  $\mu$ m and 60  $\mu$ m were adopted in the current study, to investigate the layer thickness effects on microstructure and mechanical characteristics of the AM built AlSi10Mg alloy parts. During SLM experiments, Argon gas was used to protect the melt pool. The SLM experiments were conducted under an Argon atmosphere at a constant flow rate to maintain the oxygen level below 200ppm. Fig. 1 shows schematically the SLM process.

Macro and microstructural characterizations of AM built parts were analyzed using optical microscope and high magnification SEM. Samples were cut in the transverse direction at 3 mm below from the top of the built and polished and etched based on the standard metallography procedure. Specimens were chemically etched using the keller's reagent solution.

TABLE I. CHEMICAL COMPOSITION OF ALSI10MG POWDER

Al	Si	Fe	Cu	Mn	Mg	Zn	Ti
Balance	9.0–11.0	0.3	0.03	0.001–0.4	0.2–0.5	0.1	0.15

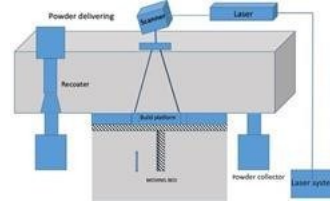


Figure 1. Schematic diagram of SLM

Hardness of the parts were accessed by utilizing a Micro- Vickers hardness tester with an applied load of 100 g and a dwell time of 10 sec. An average of indentations was taken. Further, uniaxial tensile testing was carried out with a cross- head speed of 1 mm/min. Total three tensile test specimens were accessed in each condition and the specimens were prepared based on the ASTM E8 standard.

## III. RESULTS AND DISCUSSION

### A. Powder Characteristics

As well known that the particle size distribution influences the powder flowability as well as melting behavior during processing. SEM Micrograph of AlSi10Mg powder has been depicted in Fig. 2(a). Fig. 2(b) shows the distribution of powder particle, with the size of the particle ranges from 21 $\mu$ m to 69 $\mu$ m. AlSi10Mg powder characterized to be very irregular and complex morphology. It can also be seen that the small irregular particles were connected to the large powder particles.

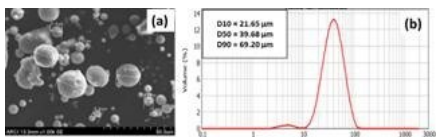


Figure 2. (a) SEM images, and (b) Particle size distribution of AlSi10Mg powder

Also, certain powder particles consist of fine internal pores which was originated during atomization process by entrapment of gases. These can significantly influence the quality of the AM built part by forming the gas pores in the AM built during solidification.

### B. Microstructural Analysis of AlSi10Mg AM built specimens

SLM process being a layer by layer melting with fast and directional cooling sequence creates an extremely fine and unique microstructures in the AM built components.

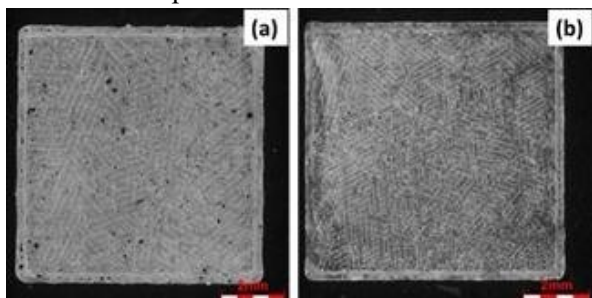


Figure 3. Top view of micro structure of AM built AlSi10Mg (a) 60  $\mu\text{m}$ (b) 30 $\mu\text{m}$

Fig 3(a) and (b) depicts the micrographs of the top section of AM built AlSi10Mg specimen built in the horizontal direction with a layer thickness of 60  $\mu\text{m}$  and 30  $\mu\text{m}$ . The porosity distribution in cross-section exhibits the top view of the AM built melt pool.

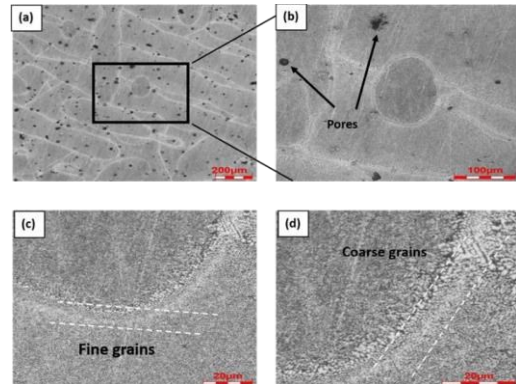


Figure 4. Optical images of AlSi10Mg @ 60  $\mu\text{m}$  layer thickness (a) microstructure @ 200X (b) Microstructure @ 693X magnification and (c) Microstructure @ 2000X magnification (d) microstructure @4000X

The microstructure was characterized by a fine dendritic microstructure Figs. 4 and 5 formed due to rapid cooling. The morphologies of the cells are different as the build layer size changes. The microstructural features of the specimens were examined and the porosity in the AM built samples with a layer thickness of 60  $\mu\text{m}$  is higher than the samples with a layer thickness of 30  $\mu\text{m}$ . It shows that the scanning direction of each layer is typically different characteristics.

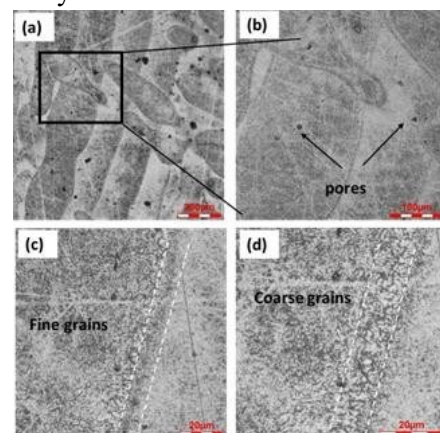


Figure 5. Optical images of AlSi10Mg @ 30  $\mu\text{m}$  layer thickness (a) Macrograph (b) Microstructure @ 200X magnification and (c) Microstructure @ 6393X magnification (d) @2700X magnification (e) @4000X magnification

### C. Mechanical properties of AM built Samples

Fig. 6 shows the tensile stress-strain curves for the AM built AlSi10Mg specimens produced with different layer thicknesses and the tensile test results are tabulated in Table

2. It has been observed that the horizontal built samples exhibit better Tensile Strength than the vertical build samples. Therefore, it can be inferred that the unique distinguishing factor for improvement in the tensile properties was sample orientation and layer thicknesses.

TABLE II. TENSILE TEST RESULTS

Specimen	Y.S (MPa)	U.T.S (MPa)	% Elong.
60 $\mu$ m-H	232	359	7.81
60 $\mu$ m-V	236	340	4.43
30 $\mu$ m-H	265	446	9.63
30 $\mu$ m-V	268	469	8.18

Results show the variation in YS and UTS between the vertical and horizontal built samples. And the UTS of 30  $\mu$ m layer thickness built specimens showed improvement in the maximum strain at failure as compared to the 60  $\mu$ m layer thickness specimens.

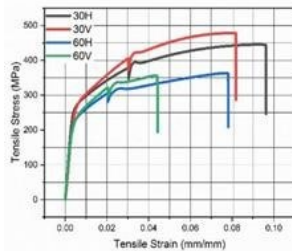


Figure 6: Tensile test results plot different layer thickness and built direction

### D. Vertical Build Direction

Tensile test values stress-strain graphs of AlSi10Mg AM built presented in Table 2 and Fig. 6 respectively. It has been observed that the elongation is significantly higher in AM samples than those mentioned in the literature values for T6 treated alloys and cast alloys. Mechanical properties of the cast alloys with heat treatment

[13, 20] and AM samples are almost the same without any remarkable difference. This improvement can be attributed to the unique fine microstructures obtained in AM process which is missing in the casting process.

### E. Horizontal Build Direction

The tensile test values stress-strain graphs of AlSi10Mg AM built presented in Table 2 and Fig. 6 respectively. It can be seen that the major difference in tensile properties of the AM built specimens in horizontal and vertical directions is the higher elongation. It can be attributed to the expected anisotropic nature of the AM built specimens which resulted due to the directional solidification of the process. In this study, it has been observed that there is no much difference in the Micro hardness of both samples with 30 $\mu$ m and 60 $\mu$ m layer thickness. So, in the additively manufactured samples, it can be concluded that the micro hardness is independent of the layer thickness.

### F. Fracture Analysis of the Tensile Specimen

The fractography method helps us majorly to improve over the process parameters selection and reduction of porosities, which in turn helps us to obtain improved characteristics using the Additive manufacturing process.

The Figs. 7 and 8 shows the magnified view in Scanning Electron Microscope of the fractured surfaces of Tensile tested AM built AlSi10Mg Tensile samples built using the SLM technique. The fractography of the tensile samples shows very rough and irregular surfaces.

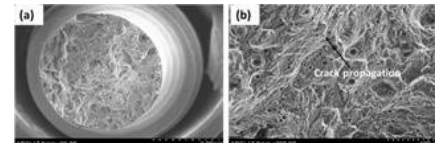


Fig 7. SEM fractography micrographs of 60 $\mu$ m horizontal built

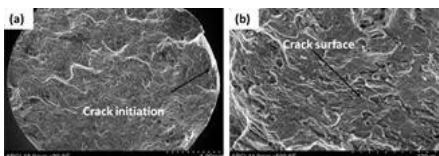


Fig 8. SEM fractography micrographs of 30µm horizontal built

Fracture morphology presented in the Figs. are characterized by the crack origin and its mode of propagation.

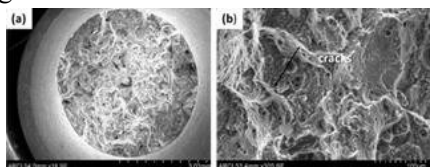


Fig 9. SEM fractography micrographs of 60µm vertical built

At higher magnification fracture surface contains unmelted powders are also seen on the surface. Images of 30µm horizontal built samples show more fibrous texture than 60µm horizontal built as the strength can be improved by reducing the layer thickness. The increase in porosity and powders left unmelted, due to the lack of solidification causing oxide layers could be the influence of the laser power, spot size, and process scanning speed.

Ductile fracture can be observed in the form of dimple present in the area of the fracture in vertical built as shown in the fig.9. In-between weakly bonded layers (Fig. 9). Due to argon gas entrapment very fine porosity can be seen. The visible Al—Si fine eutectic cellular structure and lack of un-melted powders can be observed in fig 9.

As seen in the fig.7 for horizontal built specimen's fracture surface, fine dimples, along with ridges having dense lines can be observed. The fine cellular structure is not visible here as compared to the vertical built samples. This indicates the anisotropy of the built specimens due to AM process along with the presence of

pores which is unavoidable and challenging with this process. So, in comparison to the vertical built samples, the horizontal built samples show superior elongation before fracture occurring in between the layers. The reason behind the early failure in vertical samples than horizontal samples in the presence of weakly bonded layers.

#### IV. CONCLUSION

- Since the mechanical properties (tensile strength) of the SLM AlSi10Mg samples with layer thicknesses of 60µm and 30µm that were examined here are similar, the layer thickness can be increased. The main disadvantage of AM technology is that it can lower production costs by decreasing build times as layer thickness increases.
- The Micro Vickers hardness of the two materials with 30 µm and 60 µm layer thickness (124 HV) is found to be relatively similar. Thus, it can be said that the micro hardness in the additively created AlSi10Mg samples is independent of the layer thickness.
- It has been noted that the tensile strength of the horizontally built samples is higher than that of the vertically built samples.
- The AlSi10Mg AM constructed specimens exhibit distinct microstructural characteristics and shape in both horizontal and vertical built directions.
- The 30 µm layer thickness specimens were shown to have better tensile characteristics than the 60 µm layer thickness specimens. This improvement could be attributed to factors such as improved surface shape, low porosity, and extremely fine microstructure.
-

## REFERENCES

1. N, Read; W, Wang; K, Essa.; M, Attallah: Selective laser melting of AlSi10Mg alloy: Process optimization and mechanical properties development, *Materials and Design* 65, 2015, pp. 417-424.
2. S. Romano, A. Brückner-Foit, A. Brandão, J. Gumpinger, T. Ghidini, S. Beretta: Fatigue properties of AlSi10Mg obtained by additive manufacturing: Defect-based modelling and prediction of fatigue strength, *Engineering Fracture Mechanics*, 2018, pp. 169-189.
3. E, Brandl; U, Heckenberger; V, Holzinger; D, Buchbinder: Additive manufactured AlSi10Mg samples using selective laser melting (SLM): Microstructure, high cycle fatigue, and fracture behavior. *Materials and Design* 34, 2012, pp. 159-169.
4. L, Thijs; K, Kempen; J, Kruth; J, Humbeeck: Fine-structured aluminum products with controllable texture by selective laser melting of pre-alloyed AlSi10Mg powder. *Acta Materialia* 61, 2013, pp. 1809-1819.
5. J.R. Davis, Aluminum and Aluminum Alloys, ASM Handbook, ASM International, Materials Park, 1999
6. KG, Prashanth; S, Scudino; HJ Klauss; KB, Surreddi; L, Löber; Z, Wang; AK, Choubey; U, Kühn; J, Eckert: Microstructure and mechanical properties of Al-12Si produced by selective laser melting: Effect of heat treatment. *Materials Science and Engineering A* 590, 2014, pp. 153-160.
7. NT, Aboulkhair; NM, Everitt; I, Ashcroft; C, Tuck: Reducing porosity in AlSi10Mg parts processed by selective laser melting. *Additive Manufacturing* 1-4, 2014, pp. 77-86.
8. K, Kempen; L, Thijs; J, Humbeeck; J, Kruth: Mechanical properties of AlSi10Mg produced by selective laser melting. *Physics Procedia* 39, 2012, pp. 439-446.
9. C A, Biffi; J, Fiocchia; P, Bassania; D S, Paolinob; A, Tridellob; G, Chiandussib; M, Rossettob; A, Tuissia: Microstructure and preliminary Fatigue Analysis on AlSi10Mg samples manufactured by SLM ; *Procedia Structural Integrity Volume 7*, 2017, pp. 50-57
10. J S, Zuback; T, DebRoy; The Hardness of Additively Manufactured Alloys, *Materials*, 2018; pp. 2070.
11. N, Kaufmann; M, Imran; TM, Wischeropp; C, Emmelmann; S, Siddique; F, Walther: Influence of process parameters on the quality of aluminum alloy EN AW 7075 using selective laser melting (SLM). *Physics Procedia* 83, 2016, pp.918-926.
12. H, Zhang; H, Zhu; Qi, T; Hu, Z; X, Zeng: Selective laser melting of high strength Al-Cu-Mg alloys: Processing, microstructure, and mechanical properties. *Materials Science and Engineering: A* 656, 2016, pp. 47-54.

13. M, Tang; Inclusions, Porosity, and Fatigue of AlSi10Mg Parts Produced by Selective Laser Melting; Dissertation, May 2017.
14. T. S. Srivatsan; T. S. Sudarshan, Eds., Additive Manufacturing: Innovations, Advances, 147 and Applications. CRC Press, 2015.
15. B, Stucker B, Janaki Ram G. Layer-based additive manufacturing technologies. Materials Processing Handbook: CRC Press; 2007. p. 1–32.
16. W.M. Steen, Laser material processing, 3rd edn. (Springer,Berlin, 2003), pp. 279–284
17. M. Gupta and S. Ling, Microstructure and Mechanical Properties of Hypo/Hyper-Eutectic Al-Si Alloys Synthesized Using a Near- Net Shape Forming Technique, *J. Alloys Compd.*, 1999, 287, p 284-294
18. M. Gupta, C. Lane, and E.J. Lavenia, Microstructure and Properties of Spray Atomized and Deposited Al-7SiSiCp Metal Matrix Composites, *Scr. Metall. Mater.*, 1992, 26, p 825
19. J. Hatch, Aluminum: Properties and Physical Metallurgy,American Society for Metals, Cleveland, 1984
20. EOS GmbH – Electro Optical Systems. Material Data Sheet: EOS Aluminium AlSi10Mg, [www.eos.info](http://www.eos.info), München, 2014.
21. ASTM B85, Standard Specification for Aluminum-Alloy Die Castings, ASTM International, West Conshohocken, PA, 2013
22. ASTM Committee F42, “ISO / ASTM 52900-15: Standard Terminology for Additive Manufacturing Technologies - General Principles - Terminology,” ASTM International. ASTM International, 2015.